9694 *Inorg. Chem.* **2010**, *49*, 9694–9699
DOI: 10.1021/ic1015143

Inorganic Chemistry
Article

Synthesis and Characterization of Carbonyl Diazide, $OC(N_3)_2$

Xiaoqing Zeng,[†] Michael Gerken,*,[†,‡] Helmut Beckers,[†] and Helge Willner*,[†]

[†] *Bergische Universität Wuppertal, FB C − Anorganische Chemie, Gauss Strasse 20, D-42097 Wuppertal, Germany, and* [‡] *Department of Chemistry and Biochemistry, The University of Lethbridge, Lethbridge, Alberta T1K 3M4, Canada*

Received July 28, 2010

The previously recognized “extremely explosive” carbonyl diazide, $OC(N_3)_2$, was prepared as a pure compound and unambiguously characterized by gas-phase IR, matrix IR, and Raman spectroscopy and X-ray crystallography for the first time. The pure substance shows remarkable kinetic stability at room temperature in the gaseous, liquid, and solid states. A melting point of 16 °C and vapor pressure of 5.6 mbar at 0 °C were determined. Two planar conformers were found in the gas phase, and a composition of 12% *anti*−*syn* versus 88% *syn*−*syn* conformer in the gaseous equilibrium mixture at room temperature was estimated by matrix IR spectroscopy. In the crystal structure, only the more stable *syn*−*syn* conformer was observed. The preference of the *syn*−*syn* configuration was supported by DFT calculations.

Introduction

Azides, known as a class of high-energy materials, have been widely used in various fields of chemistry.[1] Among these azides, covalent polyazides of the type $RM(N_3)_n$ are of particular interest for preparative chemists due to their high-energy content. Although they are usually rather sensitive to heat, shock, and friction, the interest in their physical and chemical properties has stimulated a large number of studies in the past decade. Recently, many exciting polyazides of group 15 (P, As, Sb)[2] and 16 (Se, Te)[3] elements have been prepared and structurally characterized. As for the group 14 element carbon, numerous organic mono- and diazides are well-known, and some of them are fairly stable at room temperature and even commercially available. Very recently, an extremely explosive polyazide of carbon, tetraazidomethane, $C(N_3)_4$, was successfully isolated and characterized by IR and NMR spectroscopy and mass spectrometry.[4]

As one of the simplest diazides of carbon, $OC(N_3)_2$, was barely known; only a few references mentioned that it was formed and used as an *in situ* reagent.[5] More recently, it was mentioned as a hydrolysis product of $C(N_3)_4$ as evidenced by ^{13}C and ^{15}N NMR spectroscopy,[4] but it has never been isolated as a pure substance up to now. It was even suggested by the authors that “it is never wise to isolate it and work with only small quantities of solution at a time”.[5a]

Herein, we described a safe way of preparing and handling $OC(N_3)_2$ as a pure substance in small quantities. Its physical properties were obtained, and a full characterization of this compound was carried out by IR (gas-phase, Ar matrix) and Raman (solid) spectroscopy and X-ray crystallography.

Experimental Section

Caution! *Covalent azides are potentially hazardous and explosive! Carbonyl diazide,* $OC(N_3)_2$*, was supposed to be an extremely explosive compound, and we found it is very shock-sensitive in the solid state. Although we did not experience any unexpected explosions during this work, safety precautions (face shields, leather gloves, and protective leather clothing) are strongly recommended, particularly in the case of handling pure* $OC(N_3)_2$ *in the solid and liquid states.*

Materials and Apparatus. Fluoro carbonyl chloride (FC(O)-Cl) was taken out of a flame-sealed glass ampule, which was stored under liquid nitrogen in a long-term Dewar vessel, and its

---

*To whom correspondence should be addressed. E-mail: michael.gerken@uleth.ca (M.G.), willner@uni-wuppertal.de (H.W.).

(1) See recent reviews: (a) Bräse, S.; Gil, C.; Knepper, K.; Zimmermann, V. *Angew. Chem., Int. Ed.* **2005**, *44*, 5188–5240. (b) Knapp, C.; Passmore, J. *Angew. Chem., Int. Ed.* **2004**, *43*, 4834–4836. (c) Tornieporth-Oetting, I. C.; Klapötke, T. M. *Angew. Chem., Int. Ed.* **1995**, *34*, 511–520.

(2) See, for example: (a) Portius, P.; Fowler, P. W.; Adams, H.; Todorova, T. Z. *Inorg. Chem.* **2008**, *47*, 12004–12009. (b) Zeng, X. Q.; Wang, W. G.; Liu, F. Y.; Ge, M. F.; Sun, Z.; Wang, D. X. *Eur. J. Inorg. Chem.* **2006**, 416–421. (c) Goebel, M.; Karaghiosoff, K.; Klapoetke, T. M. *Angew. Chem., Int. Ed.* **2006**, *118*, 6183–6186. (d) Haiges, R.; Boatz, J. A.; Vij, A.; Vij, V.; Gerken, M.; Schneider, S.; Schroer, T.; Yousufuddin, M.; Christe, K. O. *Angew. Chem., Int. Ed.* **2004**, *43*, 6676–6680.

(3) (a) Klapötke, T. M.; Krumm, B.; Scherr, M.; Haiges, R.; Christe, K. O. *Angew. Chem., Int. Ed.* **2007**, *46*, 8686–8690. (b) Klapötke, T. M.; Krumm, B.; Scherr, M. *Inorg. Chem.* **2008**, *47*, 4712–4722. (c) Haiges, R.; Boatz, J. A.; Vij, A.; Gerken, M.; Schneider, S.; Schroer, T.; Christe, K. O. *Angew. Chem., Int. Ed.* **2003**, *42*, 5847–5851. (d) Klapötke, T. M.; Krumm, B.; Polborn, K. *J. Am. Chem. Soc.* **2004**, *126*, 710–711. (e) Klapötke, T. M.; Krumm, B.; Mayer, P.; Schwab, I. *Angew. Chem., Int. Ed.* **2003**, *42*, 5843–5846. (f) Klapötke, T. M.; Krumm, B.; Mayer, P.; Piotrowski, H.; Ruscitti, O. P.; Schiller, A. *Inorg. Chem.* **2002**, *41*, 1184–1193.

(4) Banert, K.; Joo, Y.-H.; Rüffer, T.; Walfort, B.; Lang, H. *Angew. Chem., Int. Ed.* **2007**, *46*, 1168–1171.

(5) (a) Chapman, L. E.; Robbins, R. F. *Chem. Ind.* **1966**, *29*, 1266–1267. (b) Curtius, T.; Bertho, A. *Ber. Deut. Chem. Ges.* **1926**, *59B*, 565–589. (c) Kesting, W. *Ber. Deut. Chem. Ges.* **1924**, *57B*, 1321–1324.

purity was checked by IR spectroscopy. Sodium azide (Alfa Aesar) was purified according to a literature method.[6] The salt was washed and dried at 100 °C before use. For the preparation of the ^{15}N-labeled sample, 1-^{15}N sodium azide (98 atom % ^{15}N, EURISOTOP GmbH) was used as received. Volatile materials were manipulated in a glass vacuum line equipped with a capacitance pressure gauge (221 AHS-1000, MKS Baratron, Burlington, MA), three U traps, and valves with PTFE stems (Young, London, U. K.). The vacuum line was connected to an IR gas cell (optical path length 20 cm, Si windows, 0.6-mm-thick) contained in the sample compartment of the FT-IR instrument (Bruker, Vector 22), which was used for IR spectroscopic characterization of volatile products. The final products were stored in flame-sealed glass ampules in liquid nitrogen. Glass ampules were opened on the vacuum line by means of an ampule key,[7] and appropriate amounts were taken out, followed by flame-sealing the ampule with the remaining sample.

Synthesis. Carbonyl diazide, $OC(N_3)_2$, was prepared by reacting NaN_3 (0.5 mmol) with FC(O)Cl (1.4 mmol) in a flame-sealed glass ampule (i.d. 0.4 cm, o.d. 0.6 cm, length 20 cm) at room temperature for 4 days. Volatile products from three batches were collected and separated by repeated trap-to-trap condensation (−60 °C, −100 °C, −196 °C). The product (ca. 60 mg), $OC(N_3)_2$, was retained in the −60 °C trap as a white solid. The more volatile product $FC(O)N_3$ was found in the −100 °C trap as confirmed by its IR spectrum.[8] Unreacted FC(O)Cl was retained in the −196 °C trap. 1-^{15}N sodium azide was used for the ^{15}N-labeled sample in a similar manner. The quality of the samples was ascertained by gas-phase IR spectroscopy. The starting material FC(O)Cl was chosen for the synthesis of $OC(N_3)_2$ rather than $OCCl_2$ or OCF_2 because, in the first step, $FC(O)N_3$ is formed as a stable intermediate by a fast chlorine−azide substitution reaction.[8] In a second step, this monoazide undergoes a slower fluorine−azide substitution reaction to form $OC(N_3)_2$.

Vibrational Spectroscopy. Raman spectra were recorded on a Bruker-Equinox 55 FRA 106/S FT-Raman spectrometer using a 1064-nm Nd:YAG laser (200 mW) with 200 scans at a resolution of 2 cm^{-1}. For the low-temperature Raman measurement, a small amount of sample (ca. 20 mg) was condensed onto a stainless steel finger which was cooled with liquid nitrogen. Subsequently, the coldfinger was rotated under high vacuum conditions toward the laser beam. The sample was completely recovered after the measurement.

Matrix IR spectra were recorded on a FT-IR spectrometer (IFS 66v/S Bruker) in reflectance mode using a transfer optic. A KBr beam splitter and an MCT detector were used in the region of 5000 to 550 cm^{-1}. For each spectrum, 200 scans at a resolution of 0.25 cm^{-1} were coadded. The gaseous sample was mixed by passing the argon gas through a U trap containing ca. 10 mg of $OC(N_3)_2$, which was kept in an ethanol bath at a temperature of −65 °C. By adjusting the flow rate of Ar (2 mmol/h), a small amount of the resulting mixture ($OC(N_3)_2/Ar \approx 1{:}1000$ estimated) was deposited within 10 min onto the matrix support at 16 K (Rh-plated Cu block) under high vacuum conditions. Details of the matrix apparatus have been described elsewhere.[9]

UV/Vis Spectroscopy. The UV spectrum of the gas sample (0.5 mbar) was recorded in the range 200−700 nm using a quartz cell (10 cm optical path length) on a Perkin-Elmer Lambda EZ210 spectrophotometer.

Single Crystal Structure Determination. a. Crystal Growth and Crystal Mounting. Single crystals of $OC(N_3)_2$ were grown in an L-shaped glass tube (o.d. 0.6 cm, length 20 cm). Small amounts (ca. 5 mg) of the compounds were condensed at −196 °C into the upper part of the tube (above the bent), which was connected to the vacuum line and subsequently flame-sealed. The end without sample was immersed into an ethanol cold bath at ca. −65 °C, while the whole setup with the cold bath was kept in a refrigerator at −20 °C. After 3 h, colorless crystals were obtained in the bottom of the tube immersed in the cold bath. Since solid $OC(N_3)_2$ is rather sensitive to a sudden change of pressure, the transfer of the crystals *must* be done with great care, i.e., the 6-mm glass tube with crystals was kept cold in a dry ice bath (ca. −78 °C) and connected to the vacuum line. Then, the tube was opened to the vacuum with an ampule key,[7] and the tube was slowly filled with argon gas to 1 atm, followed by a quick transfer of the crystals into a trough cooled by a flow of cold nitrogen. A suitable cystal of $OC(N_3)_2$ was selected at ca. −70 °C under the microscope and mounted as previously described.[10]

b. Collection and Reduction of X-Ray Diffraction Data. Crystals were centered on an Oxford Diffraction Gemini E Ultra diffractometer, equipped with a 2K × 2K EOS CCD area detector, a four-circle κ goniometer, an Oxford Instruments Cryojet, and sealed-tube Enhanced (Mo) and the Enhanced Ultra (Cu) sources. For the data collection, the Cu source emitting monochromated Cu Kα radiation (λ = 1.54184 Å) was used. The diffractometer was controlled by the CrysAlis$^{\text{Pro}}$ Graphical User Interface (GUI) software.[11] The diffraction data collection strategy for $OC(N_3)_2$ was optimized with respect to complete coverage and consisted of 10 ω scans with a width of 1°, respectively. The data collection for $OC(N_3)_2$ was carried out at −123 °C, in a 1024 × 1024 pixel mode using 2 × 2 pixel binning. Processing of the raw data, scaling of diffraction data and the application of an empirical absorption correction was completed by using the CrysAlis$^{\text{Pro}}$ program.[11]

c. Solution and Refinement of the Structure. The solutions were obtained by direct methods which located the positions of all atoms. The final refinement was obtained by introducing anisotropic thermal parameters and the recommended weightings for all of the atoms. All calculations were performed using the SHELXTL-plus package for the structure determination and solution refinement and for the molecular graphics.[12]

Computational Details. Geometry optimizations were performed using DFT methods (B3LYP,[13] BP86,[14] MPW1PW91[15]) with the 6-311+G(3df) basis set; local minima were confirmed by harmonic frequency analyses. The complete basis set (CBS-QB3) method was used for accurate energy calculations.[16] All of the calculations were performed using the Gaussian 03 software package.[17]

---

(6) O'Neill, S. R.; Shreeve, J. M. *Inorg. Chem.* **1972**, *11*, 1629–1631.

(7) Gombler, W.; Willner, H. *J. Phys. E.: Sci. Instrum.* **1987**, *20*, 1286.

(8) Mack, H.-G.; Della Védova, C. O.; Willner, H. *J. Mol. Struct.* **1993**, *291*, 197–209.

(9) Schnöckel, H. G.; Willner, H. In *Infrared and Raman Spectroscopy, Methods and Applications*; Schrader, B., Ed.; VCH: Weinheim, Germany, 1994.

(10) Zeng, X. Q.; Gerken, M.; Beckers, H.; Willner, H. *Inorg. Chem.* **2010**, *49*, 3002–3010.

(11) *CrysAlisPro*, version 1.171.33.42; Oxford Diffraction Ltd: Oxford, U. K.

(12) Sheldrick, G. M. *SHELXTL97*, University of Göttingen: Göttingen, Germany, 1997.

(13) Becke, A. D. *J. Chem. Phys.* **1993**, *98*, 5648–5652.

(14) Perdew, J. P. *Phys. Rev. B* **1986**, *33*, 8822–8824.

(15) Adamo, C.; Barone, V. *J. Chem. Phys.* **1998**, *108*, 664–675.

(16) Montgomery, J. A., Jr.; Frisch, M. J.; Ochterski, J. W.; Petersson, G. A. *J. Chem. Phys.* **2000**, *112*, 6532–6542.

(17) Frisch, M. J.; Trucks, G. W.; Schlegel, H. B.; Scuseria, G. E.; Robb, M. A.; Cheeseman, J. R.; Montgomery, J. A., Jr.; Vreven, T.; Kudin, K. N.; Burant, J. C.; Millam, J. M.; Iyengar, S. S.; Tomasi, J.; Barone, V.; Mennucci, B.; Cossi, M.; Scalmani, G.; Rega, N.; Petersson, G. A.; Nakatsuji, H.; Hada, M.; Ehara, M.; Toyota, K.; Fukuda, R.; Hasegawa, J.; Ishida, M.; Nakajima, T.; Honda, Y.; Kitao, O.; Nakai, H.; Klene, M.; Li, X.; Knox, J. E.; Hratchian, H. P.; Cross, J. B.; Adamo, C.; Jaramillo, J.; Gomperts, R.; Stratmann, R. E.; Yazyev, O.; Austin, A. J.; Cammi, R.; Pomelli, C.; Ochterski, J. W.; Ayala, P. Y.; Morokuma, K.; Voth, G. A.; Salvador, P.; Dannenberg, J. J.; Zakrzewski, V. G.; Dapprich, S.; Daniels, A. D.; Strain, M. C.; Farkas, O.; Malick, D. K.; Rabuck, A. D.; Raghavachari, K.; Foresman, J. B.; Ortiz, J. V.; Cui, Q.; Baboul, A. G.; Clifford, S.; Cioslowski, J.; Stefanov, B. B.; Liu, G.; Liashenko, A.; Piskorz, P.; Komaromi, I.; Martin, R. L.; Fox, D. J.; Keith, T.; Al-Laham, M. A.; Peng, C. Y.; Nanayakkara, A.; Challacmobe, M.; Gill, P. M. W.; Johnson, B.; Chen, W.; Wong, M. W.; Gonzalez, C.; Pople, J. A. *Gaussian 03*, revison D.01; Gaussian, Inc.: Wallingford, CT, 2003.

Results and Discussion

Physical Properties. The physical properties and stability of $OC(N_3)_2$ are of great importance for its potential applications. Carbonyl diazide is a white solid at low temperature with a vapor pressure of 5.6 mbar at 0 °C. Vapor pressures of the solid were measured in the temperature range of −15 to 0 °C. From these vapor pressures, an empirical equation was obtained (Figure S1, Supporting Information):

$$\log p_{\mathrm{solid}} = -2085.2/T + 8.447 \ (p \text{ in mbar}, T \text{ in K})$$

It can easily be transferred by vacuum sublimation with no noticeable decomposition. However, solid $OC(N_3)_2$ is very shock-sensitive. For example, when a flame-sealed, evacuated 6-mm glass tube containing small amounts of solid carbonyl diazide (ca. 3 mg) was cracked open inside a fumehood while kept at −196 °C, an explosion with a flash of light was observed.

The melting point of $OC(N_3)_2$ was determined by condensing in vacuo approximately 5 mg of sample into the bottom of a capillary (o.d. 0.4 cm, i.d. 0.3 cm, length 20 cm). After flame-sealing the capillary above the sample cooled with liquid nitrogen, the temperature was increased at a rate of 1.0 °C/min starting at −30 °C (cold ethanol bath). The colorless solid melts sharply at 16 °C to a colorless liquid. To assess the stability of the liquid in the capillary, this sample was stored at room temperature for two weeks. Upon cooling to −65 °C, the sample solidified to a colorless solid $OC(N_3)_2$. The capillary was then cooled with liquid nitrogen and hit in the fume hood, which caused a violent explosion. Hence, gaseous and liquid $OC(N_3)_2$ was found to be stable for two weeks at room temperature.

The UV/vis spectrum of gaseous $OC(N_3)_2$ (Figure S2, Supporting Information) shows two absorption bands, similar to other covalent azides: $\lambda_{\max} = 232$ and 198 nm, which are assigned to the $n \rightarrow \pi^*$ and $\pi \rightarrow \pi^*$ transitions, respectively.

Vibrational Spectroscopy. Gas-phase and Ar matrix IR spectra, as well as a low-temperature Raman spectrum, were recorded of $OC(N_3)_2$. The IR and Raman spectra of $OC(N_3)_2$ are shown in Figure 1, and the observed band positions are listed in Table 1 and compared with the calculated frequencies of the two conformers of $OC(N_3)_2$ at the B3LYP/6-311+G(3df) level of theory. Each conformer has 18 fundamentals; 7 of these 18 modes are stretching vibrations. Besides ν(CO), ν_{as}(NCN), and ν_s(NCN) stretches, the two azide groups give rise to symmetric and asymmetric N_3 stretching modes, which are coupled and appear as in-phase and out-of-phase vibrations, resulting in overall four N_3 stretches. In-phase and out-of-phase combinations also exist for the in-plane and out-of-plane bending, rocking, and torsional modes of the two N_3 groups.

Both conformers are asymmetric rotators, and in the gas-phase IR spectrum, some bands exhibit band contours of the A-, B-, A/B-, or C-type, which allows the easy distinction between in-plane and out-of-plane vibrations. For example, the bands at 723 and 569 cm^{-1} exhibit contours with a prominent Q branch and are accordingly attributed to out-of-plane deformation modes.

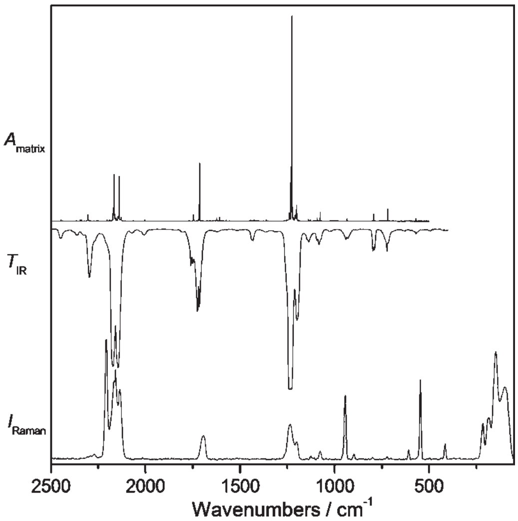

Figure 1. Upper trace: IR spectrum of $OC(N_3)_2$ isolated in an Ar matrix at 16 K (absorbance A, resolution: 0.25 cm^{-1}). Middle trace: IR spectrum of gaseous $OC(N_3)_2$ at 298 K (transmission T, resolution: 2 cm^{-1}). Lower trace: Raman spectrum of solid $OC(N_3)_2$ at 77 K (Raman intensity I, resolution: 2 cm^{-1}).

In the rotameric mixture, four bands for the asymmetric N_3 stretches are predicted around 2200 cm^{-1}. However, the agreement between observed and calculated band positions and intensities is not satisfactory, likely because of anharmonic resonances with combination modes. The next two IR bands of the gas-phase IR spectrum at 1756 and 1721 cm^{-1} exhibit B-type band contours with a PR separation of 10 cm^{-1} as expected for the two CO stretching modes. By comparison with the calculated band positions and intensities, they are attributed to the *anti−syn* and *syn−syn* conformers, respectively. Their frequency difference of 35 cm^{-1} is consistent with the calculated frequency difference for the CO stretches of the two conformers (42 cm^{-1}, B3LYP/6-311+G(3df); Table 1). The observed difference between the CO stretching frequencies of the *syn−syn* and *anti−syn* conformers of $OC(N_3)_2$ is similar to that observed between the two conformers of $FC(O)N_3$ (42 cm^{-1}).[8] An accurate estimate of the composition of the two conformers based on their CO stretches in the gas-phase IR spectrum is difficult due to overlap. In the IR spectrum of Ar matrix isolated $OC(N_3)_2$ shown in Figure 1 (upper trace), the two CO stretches associated with the two conformers are well-separated and appear at 1747.3 and 1713.0 cm^{-1}. An integration of the two band areas, including all the matrix sites, gave a ratio of 1:3.2. By taking the theoretically calculated ratio of their absorbances (2.2:1) into account, an *anti−syn*/*syn−syn* composition of 12% and 88% was derived for the two conformers at room temperature, which is the same as the predicted composition based on the difference of the calculated Gibbs free energies at 298 K (B3LYP/6-311+G(3df)) (vide infra). By heating the gas mixture of $OC(N_3)_2$/Ar prior to its deposition as a matrix, the band at 1747.3 cm^{-1} increased in intensity at the expense of that at 1713.0 cm^{-1}. Hence, the weaker band at 1747.3 cm^{-1} is attributed to the *anti−syn* conformer rather than to a combination or overtone band. The assignment of the IR bands around 1250 cm^{-1} to the four $\nu_s(N_3)$ stretching

Table 1. Experimental and Calculated Vibrational Frequencies (cm^{-1}) of $OC(N_3)_2$

experimental[a]				calculated[b]		
IR			Raman[c]	*syn-syn*	*anti-syn*	approximate mode description
vapor, 298 K	band contour, Δν(PR)[d]	Ar-matrix,[e] 15 K	solid, 77 K			
			2208 (100)			
2298 m		2305.6 m				$\nu_{as}(N_3)$
			2167 (66)	2298 (59)		
2175 vs		2166.8 s			2293(607)	
			2159 (75)	2283 (993)		
2147 vs		2139.1 s			2276 (336)	
			2137 (59)			
1756 m	B-type, 10	1747.3 m			1791 (541)	ν(CO)
1721 s	B-type, 10	1713.0 s	1695 (20)	1749 (251)		
		1239.5 w		1324 (3)		$\nu_s(N_3)$
1259 sh		1230.9 s			1315 (370)	
1235 vvs	A/B-type, 8	1225.6 vvs	1236 (29)	1293 (1453)		
1197 m		1200.8 m	1201 (14)		1285 (536)	
1139 w		1138.3 w	1126 (3)	1116 (215)		ν_{as}(NCN)
					1112 (341)	
			1077 (6)			2 × 546 = 1092
936 w		933.6 w	945 (53)	941 (23)		ν_s(NCN)
			898 (4)		889 (8)	
794 w	B-type, 10	793.1 m	800 (2)	800 (26)		NCN in-plane def.
					729 (35)	
723 w	C-type, 16	719.3 m	722 (2)	729 (23)		N_2CO out-of-plane def.
		717.5 w			720 (23)	
			608 (8)		618 (2)	N_3 out-of-plane def.
569 vw	C-type, 16	569.7 w		597 (7)	596 (2)	
				585 (< 1)		
			546 (67)	564 (< 1)	583 (8)	N_3 in-plane def.
				507 (< 1)	499 (< 1)	
			416 (13)	410 (2)	444 (1)	bending, rocking, torsional modes
			216 (31)	209 (1)	203 (2)	
			185 (56)	161 (< 1)	139 (< 1)	
			147 (90)	123 (< 1)	123 (< 1)	
				75 (< 1)	99 (< 1)	

[a] Experimental band positions and intensities: vvs, very very strong; vs, very strong; s, strong; m, medium strong; w, weak; and vw, very weak. [b] B3LYP/6-311+G(3df) level; IR intensities (km mol^{-1}) in parentheses. [c] Relative Raman intensities are given in parentheses. [d] In cm^{-1}. [e] Most intensive matrix site.

vibrations is also ambiguous due to possible disturbances by combination modes. The expected satellites at ν_{as} and ν_s(NCN) of the *anti*−*syn* conformer are too weak to be detected. All modes below 590 cm^{-1} are strongly mixed and are difficult to describe.

The Raman spectrum of $OC(N_3)_2$ in the solid state at −196 °C shows one broad band at 1695 cm^{-1} for the CO stretch, and the other major bands can also be satisfactorily assigned to the *syn*−*syn* conformer. The appearance of two weak bands at 898 and 608 cm^{-1} suggests the existence of the *anti*−*syn* conformer in the solid that was deposited of gaseous $OC(N_3)_2$ at −196 °C.

In order to aid the vibrational assignment, matrix IR spectra of a ^{15}N labeled sample were recorded. The calculated and experimental isotopic shifts are listed in Tables S1 and S2, Supporting Information. While the lower-frequency bands are in excellent agreement between the experimental and calculated isotropic shifts, analyses of the symmetric and asymmetric N_3 stretching bands are difficult, due to extensive overlap, the presence of matrix-site splittings, and extensive disturbance by anharmonic resonances.

Crystal Structure. Carbonyl diazide crystallizes in the orthorhombic space group *Pnma* with four molecules per unit cell (Table 2). The molecular structure is shown in Figure 2, and the structural parameters are listed in Table 3.

The molecule adopts crystallographic C_s symmetry with all the atoms in one plane. The two azide groups are oriented in the *syn* position to the C=O bond with respect to the two C−N bonds, and they are the same within 3σ. The C=O bond length of 1.200(6) Å is much shorter than that of $OC(NH_2)_2$ (1.258(1) Å, neutron diffraction),[18] consistent with the electron withdrawing abilities of the substituents. The two C−N bonds are 1.407(8) and 1.412(7) Å, slightly longer than that of the monoazide $FC(O)N_3$ (1.390(4) Å) as determined by gas electron diffraction.[8]

---

[18] Swaminathan, S.; Craven, B. M.; McMullan, R. K. *Acta Crystallogr.* **1984**, *B40*, 300–306.

Table 2. Summary of Crystal Data and Refinement Results for $OC(N_3)_2$

chemical formula	CN_6O
space group	*Pnma* (No. 62)
a (Å)	5.431(2)
b (Å)	5.797(2)
c (Å)	13.800(4)
α (deg)	90
β (deg)	90
γ (deg)	90
V (Å^3)	434.5(3)
Z (molecules/unit cell)	4
mol wt	112.07
calcd density (g cm^{-3})	1.713
T (°C)	−123
μ (mm^{-1})	1.318
R_1[a]	0.0588
wR_2[b]	0.2180

[a] R_1 is defined as $\sum||F_o| - |F_c||/\sum|F_o|$ for $I > 2\sigma(I)$. [b] wR_2 is defined as $[\sum[w(F_o^2 - F_c^2)^2]/\sum w(F_o^2)^2]^{1/2}$ for $I > 2\sigma(I)$.

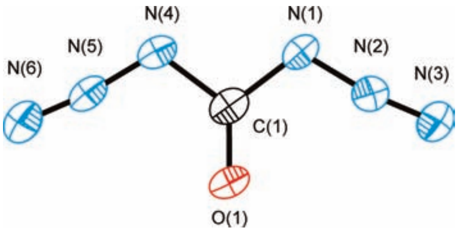

Figure 2. Molecular structure of $OC(N_3)_2$ as determined by X-ray crystallography with thermal ellipsoids at the 50% probability level.

Table 3. Calculated and Experimental Structures of $OC(N_3)_2$

	calculated[b]		experimental
parameters[a]	*anti−syn* (C_s)	*syn−syn* (C_{2v})	X-ray crystallography
R(C1−O1)	1.196	1.203	1.200(6)
R(C1−N1)	1.425	1.408	1.407(8)
R(C1−N4)	1.404	1.408	1.412(7)
R(N1−N2)	1.242	1.243	1.274(7)
R(N2−N3)	1.118	1.118	1.111(7)
R(N4−N5)	1.243	1.243	1.265(7)
R(N5−N6)	1.120	1.118	1.111(6)
∠(O1C1N1)	125.7	126.5	127.2(5)
∠(O1C1N4)	122.1	126.5	127.2(5)
∠(C1N1N2)	114.2	114.2	111.5(4)
∠(C1N4N5)	117.8	114.2	111.8(4)
∠(N1N2N3)	174.7	173.4	172.1(5)
∠(N4N5N6)	171.9	173.4	172.6(6)

[a] Bond lengths and angles are given in Å and deg, respectively. For labeling of atoms, see Figure 3. [b] Calculated values at the B3LYP/6-311+G(3df) level of theory; molecule symmetry is given in parentheses.

Quantum Chemical Calculations. Full optimizations of all possible conformers on the potential energy surface of $OC(N_3)_2$ were performed using DFT methods of B3LYP, BP86, MPW1PW91, and CBS-QB3. Only two conformers, denoted as *anti−syn* and *syn−syn* (Figure 3), were found to be true minima. The *anti*/*syn* notation refers to an *anti*/*syn* conformation of the azide group to the C═O group with respect to the C−N bond. A third planar conformer where the two N_3 groups are both in the *anti* configuration to the C═O bond was proven not to be a minimum with the occurrence of one imaginary frequency, which is probably due to the repulsive interactions between the two N_3 groups.

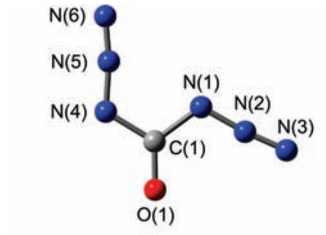

anti-syn

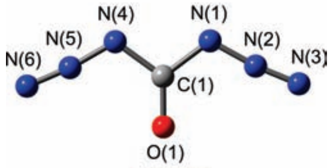

syn-syn

Figure 3. Calculated structures of $OC(N_3)_2$.

Table 4. Calculated Relative Total Energies (Δ*E*, kJ mol^{-1}), Gibbs Free Energies (Δ*G*, kJ mol^{-1}) of the *anti−syn* to the *syn−syn* Conformers of $OC(N_3)_2$, and the Content of the *anti−syn* Conformer at 298 K

method	Δ*E*	Δ*G*	content (*anti−syn*)
B3LYP/6-311+G(3df)	6.9	4.99	11.9%
BP86/6-311+G(3df)	5.1	3.15	22.0%
MPW1PW91/6-311+G(3df)	6.8	4.86	12.5%
CBS-QB3	6.4	4.27	15.3%

The calculated energies of the two conformers and estimated isomeric composition are given in Table 4, and the *syn−syn* conformer was found to be slightly more stable than the *anti−syn* one with energy differences less than 7 kJ mol^{-1} at all four considered DFT levels. According to the calculated Gibbs free energy difference between the two conformers (ΔG = 4.99 kJ mol^{-1}) at the B3LYP/6-311+G(3df) level, contents of 11.9% *anti−syn* conformer in the gas phase of $OC(N_3)_2$ can be estimated at 298 K, which represents the best agreement with the experimental content of 12% *anti−syn* conformers as estimated by matrix IR spectroscopy. Thus, it can be safely concluded that the carrier of the IR band with a higher CO stretching frequency (gas-phase 1756 cm^{-1}, Ar matrix 1747.3 cm^{-1}) is the *anti−syn* conformer, while the IR band with lower CO stretching frequency (gas-phase 1721 cm^{-1}, Ar matrix 1713.0 cm^{-1}) is assigned to the more stable *syn−syn* conformer.

The preference of the *syn−syn* configuration can be attributed to a delocalization of the σ lone pairs at both α-nitrogen atoms ($n(N_\alpha)$), N1 and N4, to the σ^*(OC) orbital, leading to a planar π-conjugating system in the *syn−syn* conformer. In the *anti−syn* conformer, only the lone pair at N1 can be effectively delocalized into σ^*(OC). On the basis of these assumptions, a longer C−O bond is expected in the *syn−syn* conformer than that in the *anti−syn* one, as confirmed by theoretical calculations (*syn−syn* 1.203 Å, *anti−syn* 1.196 Å) as well as experimental observation of a higher CO stretching frequency associated with the *anti−syn* conformer than that with the *syn−syn* conformer (Table 1).

Conclusions

The previously recognized “extremely explosive” carbonyl diazide, $OC(N_3)_2$, was prepared as a pure compound and characterized by gas-phase IR, matrix IR, and Raman spectroscopy and X-ray crystallography for the first time. It was found to be rather shock-sensitive in the condensed phase, but it showed remarkable thermal stability without decomposition in the gas phase, liquid, and solid states. The solid melts at 16 °C and can easily be transferred by vacuum sublimation. Two conformers were observed in the gas phase and also in an Ar matrix by IR spectroscopy, while only one conformer, in which both N_3 groups are in a *syn* configuration to the C=O bond with respect to the two C−N bonds, was observed in the solid state. The structure of *syn*−*syn*-$OC(N_3)_2$ was determined by low-temperature X-ray crystallography. The preference of the *syn*−*syn* configuration was further supported by DFT calculations.

Acknowledgment. X.Z. expresses his thanks to the Alexander von Humboldt Foundation for a research grant. H.B. and H.W. acknowledge support from the Deutsche Forschungsgemeinschaft and the Fonds der Chemischen Industrie, and M.G. acknowledges the University of Lethbridge for granting a study leave.

Supporting Information Available: Vapor-pressure curve of solid $OC(N_3)_2$ (Figure S1); UV spectrum of $OC(N_3)_2$ (Figure S2); matrix IR spectra of ^{15}N-labeled $OC(N_3)_2$ in the frequency ranges 800−680 cm^{-1} (Figure S3), 950−890 cm^{-1} (Figure S4), and 1100−1050 cm^{-1} (Figure S5); experimental and calculated ^{15}N isotopic shifts of $OC(N_3)_2$ (Table S1, S2); and the X-ray crystallographic file in CIF format for the structure determination of $OC(N_3)_2$. This material is available free of charge via the Internet at http://pubs.acs.org.